Changes in selection pressure can facilitate hybridization during biological invasion in a Cuban lizard

Dan G. Bock[a,1,2], Simon Baeckens[b], Jessica N. Pita-Aquino[c], Zachary A. Chejanovski[c], Sozos N. Michaelides[d], Pavitra Muralidhar[e], Oriol Lapiedra[f], Sungdae Park[g], Douglas B. Menke[g], Anthony J. Geneva[h], Jonathan B. Losos[a,i,2,3], and Jason J. Kolbe[c,3]

[a]Department of Biology, Washington University in St. Louis, St. Louis, MO 63130; [b]Functional Morphology Lab, Department of Biology, University of Antwerp, B-2610 Wilrijk, Belgium; [c]Department of Biological Sciences, University of Rhode Island, Kingston, RI 02881; [d]Department of Biology, Concordia University, Montreal, QC H4B 1R6, Canada; [e]Center for Population Biology and Department of Evolution and Ecology, University of California, Davis, CA 95616; [f]CREAF (Centre for Research on Ecology and Applied Forestry), Cerdanyola del Valles, Catalonia 08193, Spain; [g]Department of Genetics, University of Georgia, Athens, GA 30602; [h]Department of Biology and Center for Computational and Integrative Biology, Rutgers University, Camden, NJ 08102; and [i]Living Earth Collaborative, Washington University in St. Louis, St. Louis, MO 63130

Contributed by Jonathan B. Losos, August 28, 2021 (sent for review May 9, 2021; reviewed by Daren C. Card and Michael D. Shapiro)

Hybridization is among the evolutionary mechanisms most frequently hypothesized to drive the success of invasive species, in part because hybrids are common in invasive populations. One explanation for this pattern is that biological invasions coincide with a change in selection pressures that limit hybridization in the native range. To investigate this possibility, we studied the introduction of the brown anole (*Anolis sagrei*) in the southeastern United States. We find that native populations are highly genetically structured. In contrast, all invasive populations show evidence of hybridization among native-range lineages. Temporal sampling in the invasive range spanning 15 y showed that invasive genetic structure has stabilized, indicating that large-scale contemporary gene flow is limited among invasive populations and that hybrid ancestry is maintained. Additionally, our results are consistent with hybrid persistence in invasive populations resulting from changes in natural selection that occurred during invasion. Specifically, we identify a large-effect X chromosome locus associated with variation in limb length, a well-known adaptive trait in anoles, and show that this locus is often under selection in the native range, but rarely so in the invasive range. Moreover, we find that the effect size of alleles at this locus on limb length is much reduced in hybrids among divergent lineages, consistent with epistatic interactions. Thus, in the native range, epistasis manifested in hybrids can strengthen extrinsic postmating isolation. Together, our findings show how a change in natural selection can contribute to an increase in hybridization in invasive populations.

invasive species | hybridization | *Anolis* | natural selection | sex chromosome

Evolutionary change can affect the success of invasive species. This possibility has been considered by biologists for more than half a century (1). Recent decades, however, have seen a remarkable growth in research on this topic (2–5), simultaneous with the greater emphasis on contemporary evolution driving ecological phenomena (6, 7). It is now widely accepted that substantial evolution can occur over a few generations, well within the timeframe in which the establishment and spread stages of biological invasions play out (6, 7).

Among evolutionary factors that can facilitate invasions, hybridization is noteworthy for several reasons (8–10). For one, hybridization between species or among lineages within species has repeatedly been observed in genetic surveys of invasive taxa. As a result, invasive populations often show levels of genetic diversity equal to or larger than those in native populations (11–14). Also, metaanalyses have shown that invasive hybrids are frequently larger and more fecund than their parents (15). Moreover, genetically, hybridization can contribute to invasive spread through hybrid vigor or adaptive introgression (12, 13, 16).

Nonetheless, studies directly connecting hybridization to invasive spread are still in the minority. As a result, we do not know how often hybridization is a true driver of invasion success, or a consequence of propagule pressure and repeated introductions of allopatric lineages (10). Furthermore, why hybridization is less common in the native range than in the invasive range of some species is unclear, particularly when opportunities for human-mediated interpopulation dispersal and contemporary physical barriers to natural dispersal do not clearly differ between ranges (e.g., refs. 14 and 17).

Changes in natural selection that occur during biological invasions may provide part of the answer for why hybrids are more common in invasive populations, especially when biological invasions occur in disturbed habitats or in habitats that are ecologically novel from the perspective of the invader. In a landmark paper on hybridization and invasiveness, Ellstrand and Schierenbeck (9)

Significance

Hybridization is common in invasive species and can be important for their success. The connection between hybridization and bioinvasions could result in part because of a disruption in the selection pressures that limit hybridization in the native range. We demonstrate that, in the lizard *Anolis sagrei*, hybridization is rare in native populations, which show frequent evidence of natural selection at a large-effect X chromosome locus. Conversely, little selection at this locus was detected in invasive populations, which do not experience large-scale contemporary gene flow, but instead maintain a mosaic of hybrid ancestries formed during invasive range colonization. Ecological changes during biological invasions can affect hybridization frequency and stability, which can in turn drive the success of invasive taxa.

Author contributions: D.G.B., J.B.L., and J.J.K. designed research; D.G.B., S.B., J.N.P.-A., Z.A.C., S.N.M., P.M., S.P., D.B.M., and A.J.G. performed research; D.G.B. analyzed data; and D.G.B., S.B., S.N.M., P.M., O.L., D.B.M., A.J.G., J.B.L., and J.J.K. wrote the paper.

Reviewers: D.C.C., Harvard University; M.D.S., University of Utah.

The authors declare no competing interest.

[1]Present address: Centre for Biodiversity Genomics, University of Guelph, Guelph, ON N1G 2W1, Canada.

[2]To whom correspondence may be addressed. Email: dan.g.bock@gmail.com or losos@wustl.edu.

[3]J.B.L. and J.J.K. contributed equally to this work.

This article contains supporting information online at https://www.pnas.org/lookup/suppl/doi:10.1073/pnas.2108638118/-/DCSupplemental.

Published October 15, 2021.

discussed 28 species for which hybridization preceded invasive spread. All of these were found to occur in habitats characterized by disturbance, indicating that the change of selection pressures experienced by parental lineages or the opening of new niches to which hybrids are better adapted might facilitate hybridization in invasive species (9). Originally proposed by Anderson (18), the possibility that unstable, rapidly changing, or novel habitats promote hybridization is now well documented in noninvasive species (19). Particularly compelling examples come from long-term field studies that show a lack of hybridization before the environment changes (20) or a return to nonhybrid status once the ancestral environment is restored (21). In a similar way, hybrids may more easily form or persist in invasive populations when biological invasions coincide with a temporary or permanent change in patterns of adaptation that evolved in the native range (22, 23).

To investigate whether changes in selection may facilitate hybridization during biological invasions, we studied the Cuban brown anole (*Anolis sagrei*), an excellent organism for such research for multiple reasons. First, it is one of the best-known examples of hybridization occurring during biological invasion. Previous studies indicated that most invasive populations in Florida, in the southeastern United States, derive from admixture between divergent native-range lineages (11, 24). Second, *A. sagrei* is a highly successful invader. Since the mid- to late-1800s, when the first populations were established in Florida, the species has colonized the entire peninsula and expanded to the north and west (11). From there, it has since seeded secondary invasions globally (11). Third, niche structure, natural selection, and local adaptation are exceptionally well-studied in anoles, thanks to decades of observational and experimental work (25). A number of these studies focused on natural and experimental populations of *A. sagrei* in its native range in the Caribbean, predominantly on islands in the Bahamas (e.g., refs. 26–33). As such, an important baseline regarding phenotypic and environmental components of native range local adaptation is available in this system.

Results and Discussion

Genetic Structure and Genetic Diversity in Native and Invasive *A. sagrei*. We first aimed to understand how genetic variation is partitioned among native and invasive populations. For the native range, we included 10 populations, 9 of which are representative of lineages known to have seeded the Florida invasion (11). For the invasive range, we included 34 populations predominantly from Florida (*SI Appendix*, Fig. S1 and Dataset S1). We obtained genome-wide SNPs for all lizards (n = 824) via reduced representation sequencing, using double digest restriction-site associated DNA sequencing (*SI Appendix*, *Supplemental Methods*). Principal component analyses (PCA), phylogenetics, and Bayesian clustering all pointed toward strong genetic structure in the native range producing six main lineages, with limited evidence of among-lineage genetic exchange (Fig. 1 *A* and *B* and *SI Appendix*, Figs. S2–S4). Specifically, only 1 of the 134 genotypes was clearly a hybrid (Fig. 1*A*). Further genetic structure was apparent within clades, albeit to a lesser extent (Fig. 1*A*, *Inset*).

Previous studies have indicated that geographical distance is an important determinant of genetic structure for *A. sagrei* in Cuba (34, 35). Our results reinforce these findings by providing evidence of strong isolation-by-distance (IBD; Mantel's $r = 0.88$, $P = 5 \times 10^{-4}$) (*SI Appendix*, Fig. S6*A*). However, contrary to expectations under true IBD, genetic distances did not increase uniformly with geographic distance. Rather, moderate within-clade genetic structure was complemented by much stronger among-clade genetic subdivisions (*SI Appendix*, Fig. S6*A*). Similar hierarchical genetic structure has been shown to lead to significant IBD (36). Strong among-clade genetic fragmentation has been found in the native range of other anole species that, like *A. sagrei*, have a broad and continuous distribution (discussed in ref. 25). The fact that some of the genetic breaks, including those described in Cuban *A. sagrei*, overlap in different species while also corresponding to inferred past geological barriers (35), suggests that they resulted from divergence in allopatry, likely during periods of partial island submergence (35, 37).

The mechanisms that allow these genetic subdivisions to be maintained in the absence of contemporary geographical barriers are, however, unknown. This genetic differentiation is particularly striking given that *A. sagrei* clades have geographically abutting distributions in Cuba (35). One possibility is that local adaptation and resulting ecological selection against immigrants and hybrids is involved. Such ecological structuring of genetic variation across the landscape is suggested by results from previous studies that indicated ecology has an important role in shaping spatial genetic divergence in anoles, albeit to a lesser extent as compared to geographical distance (34). We revisit the contribution of local adaptation below.

Compared to the native range, population structure in the invasive range was markedly different. There was no clear grouping of genotypes in PCA space (Fig. 1*A*), and all populations showed evidence of admixture, deriving ancestry from more than one native Cuban lineage (Fig. 1*B* and *SI Appendix*, Figs. S3 and S5). Also, within-population estimates of relatedness were more similar to among-population estimates of relatedness in the invasive range than in the native range, indicating that ancestral population structure has collapsed during invasion (*SI Appendix*, Fig. S7). Finally, the strength of IBD was much reduced relative to the native range (Mantel's $r = 0.28$, $P = 0.004$) (*SI Appendix*, Fig. S6*B*), as expected given that dispersal of invasive *A. sagrei* occurred with the contribution of human-mediated long-distance transport.

Shifts in genetic structure between the native and invasive ranges were accompanied by important changes in genetic variation. Genome-wide heterozygosity, which we used as a proxy for neutral genetic variation, was almost completely nonoverlapping between the two ranges, with invasive populations significantly more diverse (two-sided Wilcoxon rank-sum test, $P = 4.719 \times 10^{-9}$) (Fig. 1*C* and *SI Appendix*, Fig. S8*A*). This pattern was reversed for SNPs predicted to be detrimental: those that produce premature stop codons, frameshift mutations, or the loss of start codons (*SI Appendix*, *Supplemental Methods*). Invasive populations showed a lower proportion of these putatively deleterious mutations as compared to native populations (two-sided Wilcoxon rank-sum test, $P = 0.015$) (Fig. 1*C* and *SI Appendix*, Fig. S8*B*), indicating that the purging of genetic load occurred more readily in the invasive range. This could have happened if invasion was accompanied by a change in the fitness landscape, such that weakly deleterious alleles in native populations are more readily visible to selection in the new environment (38). As well, if recessive, even strongly deleterious alleles would have persisted at low frequency in native populations. These rare alleles should have been preferentially lost during genetic bottlenecks that occurred when invasive populations were seeded.

Invasive Genetic Structure Has Stabilized to a Mosaic of Hybrid Ancestries. The observation of widespread hybridization in invasive *A. sagrei* is notable given that hybrids among divergent lineages are rare in the native range. To investigate whether this is due to the more recent history of *A. sagrei* in Florida, such that removal of hybrids in these populations is ongoing, we resampled a subset of invasive populations 15 y after they were first sampled. We included SNPs from six Florida populations (n = 172) that we surveyed in both 2003 and 2018 (*SI Appendix*, Fig. S9).

We found that hybrid ancestry is not eliminated in Florida, and that genetic differences among populations resulting from independent introduction and hybridization events are maintained over at least 15 y. First, genetic structure inferred using PCA did not change between 2003 and 2018 (*SI Appendix*, Fig. S10*A*). Second, while populations differed in the proportion of western Cuba ancestry ($F_{5,\ 165} = 217.4$; $P < 2 \times 10^{-16}$) (*SI Appendix*, Fig. S10*B*), reflecting the mosaic of hybrid origins that

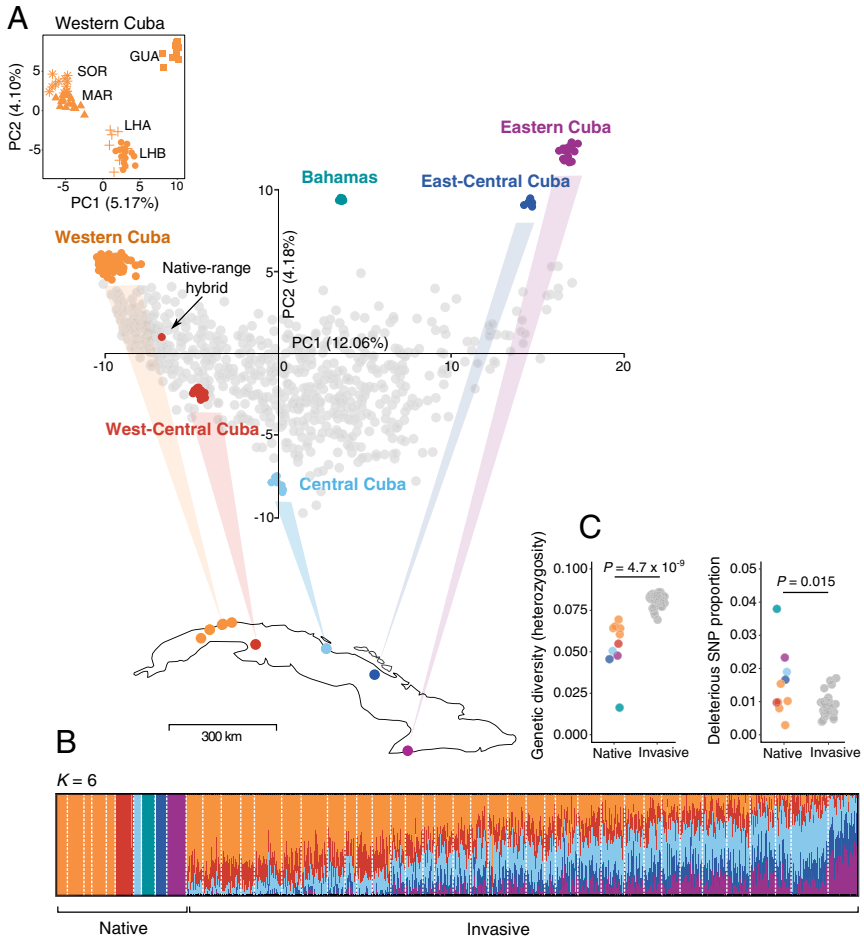

Fig. 1. Spatial genetic structure and diversity of *A. sagrei*. (*A*) PCA of all samples, and a separate PCA of the western Cuba native range subset (*Inset*). Native genotypes are in color, invasive genotypes are in gray. The arrow points to one genotype identified as a hybrid in the native range. (*B*) STRUCTURE membership, with samples grouped by range and population. Each of the 44 populations is separated by white dotted lines. With the exception of one sample that showed evidence of admixture, all native range genotypes are treated as learning samples (*SI Appendix, Supplemental Methods*). Cuba populations are arranged from west to east. Invasive populations are arranged in decreasing order of western Cuba ancestry. (*C*) Heterozygosity rate and deleterious SNP proportion, averaged per population. *P* values are from two-sided Wilcoxon rank-sum tests.

occur across Florida (Fig. 1*B*) (see also ref. 11), each population maintained similar proportions over the 15-y period ($F_{1,\ 165}$ = 0.207; P = 0.649) (*SI Appendix*, Fig. S10*B*). Third, there was no effect of sampling time on the index of admixture ($F_{1,\ 165}$ = 0.972; P = 0.325) (*SI Appendix*, Fig. S10*C*), which takes into account the contribution of each native-range lineage to the ancestry of hybrids (12).

The only metric that did change was heterozygosity, which decreased significantly over the 15 y across all populations ($F_{1,\ 165} = 50.72$; $P = 3.12 \times 10^{-11}$) (*SI Appendix*, Fig. S11*A*). Two lines of evidence suggest that this drop in heterozygosity is not a result of ongoing purging of common intrinsic incompatibilities, but is instead driven by the loss of rare alleles, likely due to genetic drift. First, heterozygosity decreased irrespective of whether hybrids originated from closely related or distantly related lineages (*SI Appendix*, Fig. S11*B*). This is inconsistent with selection against intrinsic incompatibilities, which should be more common in hybrids among divergent lineages (39). Second, polymorphism lost in the 2018 samples involved alleles that were already rare in 2003 (*SI Appendix*, Fig. S11*C*), consistent with genetic drift. We note, however, that these results do not exclude the possibility that any intrinsic incompatibilities have been purged by selection prior to 2003, the first timepoint represented in our sampling.

The finding that genetic differences established among Florida populations by 2003 remain unchanged by 2018 argues against large-scale ongoing gene flow in the invasive range. Such gene flow would have been expected to shift population genetic structure over the span of 15 y. Rather, a more plausible interpretation for hybrid ancestry in Florida populations is that distinct hybridization events took place during the evolutionary history of invasive *A. sagrei*. These hybridization events would have occurred when divergent lineages met after repeated introductions from Cuba and following progressive range expansion from these points of initial introduction.

An equally important finding is that hybrid ancestry is not only common, but it is also stable in the invasive range. This contrasts with observations in the native range where hybrids are much rarer, particularly among lineages that are representative of major phylogenetic splits in *A. sagrei*, and even when these lineages have geographically abutting distributions (e.g., the central Cuba and east-central Cuba lineages) (*SI Appendix*, Fig. S2). Limited genetic exchange among these divergent lineages in the native range is supported by our data, as well as a previous study that surveyed more Cuban populations (35). Differences in hybridization frequency between the native and invasive ranges suggest that at least some gene-flow barriers in the native range are conditional on

environment (i.e., they are extrinsic). If barriers to gene flow were predominantly unconditional (i.e., represented by intrinsic genetic incompatibilities), we would have expected to find that hybridization is equally rare in both ranges or that hybrid ancestry present in invasive populations is progressively eliminated.

Genome Scans Are Consistent with Changes in Natural Selection. To understand differences in hybridization frequency between ranges, we focused on local adaptation, which can limit gene flow between populations that inhabit different environments (40, 41). To this end, we contrasted the genomic signature of selection for the native and invasive ranges. In the native range, population differentiation was strongest on the X chromosome, where fixed differences (F_{ST} = 1) occurred even among closely related populations, for which median genome-wide F_{ST} was over 26 times lower than on the X chromosome (F_{ST} = 0.038) (Fig. 2*A* and *SI Appendix*, Fig. S12). High X chromosome F_{ST} windows were concentrated in a region of 18 Mbp in size (chromosome 7 coordinates 70 Mbp to 88 Mbp) (Fig. 2*B*). While representing 16% of the X chromosome length, this locus accounted for 47% of all X chromosome outliers and 62% of extreme X chromosome outliers.

Compared to the native range, genome-wide F_{ST} in the invasive range was only a third as high (Fig. 2*A*) and there were no fixed differences among sampling sites (all windowed F_{ST} < 1) (*SI Appendix*, Fig. S13). Even so, the genomic landscape was similar to the one we observed in the native range, with the X chromosome contributing more to population differentiation (Fig. 2*A* and *SI Appendix*, Fig. S13). Compared to the native range, however, the largest X chromosome F_{ST} peaks resulted

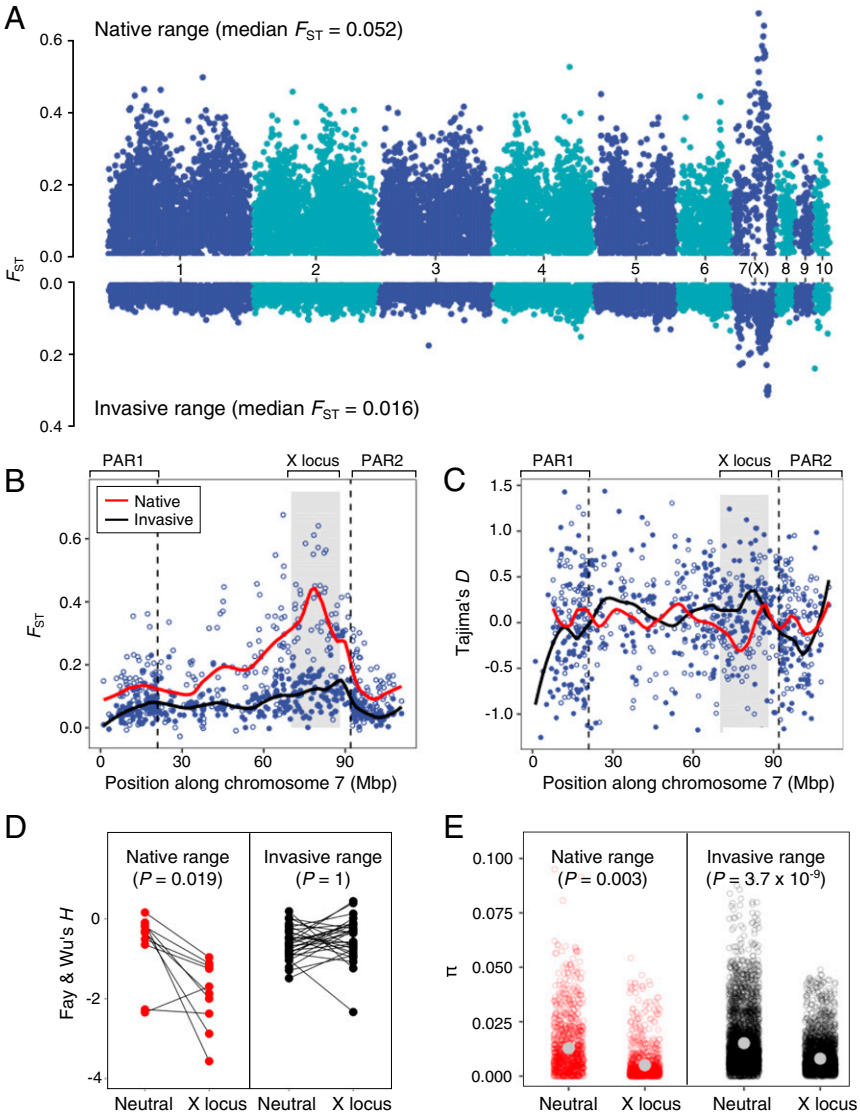

Fig. 2. Genome scans for selection. (*A*) Average genome-wide F_{ST} for the native range (*Upper*) and the invasive range (*Lower*) for chromosomes 1 to 10. (*B*) Zoomed-in view of average F_{ST} along the X chromosome (chromosome 7). (*C*) Zoomed-in view of Tajima's *D* along the X chromosome, averaged for windows with Tajima's *D* estimates at 50% or more of populations within each range. For both *B* and *C*, empty circles are used for the native range and filled circles are used for the invasive range. Colored lines show a loess smoothing ("span" of 0.2) for the native range (red) and the invasive range (black). The gray shading marks the 18-Mbp X chromosome locus where most native-range F_{ST} outliers are located (*SI Appendix*, Fig. S12). The dashed vertical lines indicate the boundaries of the PARs. (*D*) Fay and Wu's *H*, calculated within the X locus and at a region outside of this locus, used to estimate background neutral *H* levels. Lines connect *H* estimates obtained for the same population. (*E*) π Values for genomic windows within the divergent X locus and for background neutral values. Gray dots show global average π. For both *D* and *E*, *P* values are from paired Wilcoxon rank-sum tests, using averages estimated per population and locus category (*Methods*).

from comparisons among divergent lineages (*SI Appendix*, Fig. S13), which we could infer for invasive hybrids at this chromosomal region due to reduced recombination (*SI Appendix*, *Supplemental Methods*). This indicates that introduction history, which can create sharp breaks in allele frequencies among populations (42), likely has an important role in elevating invasive range F_{ST} at this genomic region. Specifically, because this locus is frequently differentiated among native-range populations, any two invasive populations with X chromosome haplotypes of different origins will also show high X chromosome F_{ST}. Finally, outliers were less concentrated in the divergent X chromosome region identified from native populations (Fig. 2*B*). In invasive populations, this locus contained 35% of all X chromosome outliers and 43% of extreme X chromosome outliers. After accounting for introduction history by excluding comparisons made among divergent X chromosome lineages, these estimates dropped to 19% and 25%, respectively.

We next asked whether the same outliers have repeatedly contributed to differentiation among independent population pairs from within either the native or the invasive ranges. Nonparallel F_{ST} windows accounted for the majority of outliers (85.4 to 89.2%) (*SI Appendix*, Table S1). While representing a smaller fraction of the genome, repeated outliers were more common than expected by chance for both ranges ($P < 0.001$ all permutation tests) (*SI Appendix*, Fig. S14). Also, relative to null expectations, there were more repeated outliers in the invasive range than in the native range (*SI Appendix*, Fig. S14). Repeated F_{ST} differentiation in both ranges is consistent with divergence under natural selection. In the invasive range, higher repeatability can be the result of the increased linkage disequilibrium that characterizes these populations (*SI Appendix*, Fig. S15), thereby enhancing nonindependence of adjacent genomic windows. While the genome-wide proportion of repeated outliers was larger in invasive populations, this pattern was reversed at the X chromosome locus, which contributed proportionately more to parallel differentiation in the native range (*SI Appendix*, Fig. S16). This further underscores that the genetic basis of population differentiation is different between the two ranges, with the X chromosome locus having a larger contribution in the native range.

In support of F_{ST} results, we found that Tajima's D is often reduced at the same X chromosome locus in native populations, but rarely so in invasive populations (Fig. 2*C* and *SI Appendix*, Figs. S17 and S18). Reduced Tajima's D indicates an excess of low-frequency variants, as expected after positive or negative selection (43). Among these possibilities, positive selection was likely involved, as indicated by Fay and Wu's H test (Fig. 2*D*). This metric quantifies the excess of derived (i.e., nonancestral) alleles, which is expected under positive selection. We found that H was lower in the native range than in the invasive range at the X chromosome divergent locus (one-sided Wilcoxon rank-sum test, $P = 1.26 \times 10^{-6}$). Also, H estimates at this genomic region were lower than background neutral values only for native populations (Fig. 2*D*), consistent with positive selection in the native range only. Background neutral H values were similar between the native and invasive ranges (one-sided Wilcoxon rank-sum test, $P = 1$), indicating that admixture or demography, which should impact genetic variation more broadly rather than a single locus, are unlikely to be a major source of bias in our results. Moreover, positive selection should have been easy to identify using Fay and Wu's H in invasive populations, because this metric has more power in admixed than in nonadmixed populations (44). Finally, we note that while analyses presented above focused on the most recent (i.e., 2018) samples from the invasive range, we also contrasted H between the 2003 and 2018 timepoints, for the six invasive populations with temporal data. These analyses provided no evidence of change in H values in the invasive range, at least over the span of the 15 y covered in our sampling (Wilcoxon rank-sum tests, all $P > 0.05$).

Compared to metrics discussed above, the signature of selection persists in nucleotide diversity (π) and absolute differentiation (D_{xy}) for more generations (45, 46). Therefore, π and D_{xy} can be informative with regards to whether selection also occurred in the common ancestor of populations under investigation. Consistent with a "selective sweep before selective population differentiation" model (47, 48), we found that both metrics tend to be reduced at the same X-linked locus relative to the rest of the chromosome in both ranges (Fig. 2*E* and *SI Appendix*, Figs. S19–S22). These findings highlighting an important role of this locus to local adaptation in the native range, and at multiple points throughout the evolutionary history of *A. sagrei*.

In summary, we find that the genomic signature of selection is different between the two ranges. In the native range, an X chromosome locus frequently retains a signature consistent with positive selection. By contrast, the same genomic region is evolving neutrally in most invasive populations. Two nonmutually exclusive explanations can account for these results. First, if evolution in both ranges is driven by similar selective forces, changes in the genomic target of selection could have occurred in invasive populations, following hybridization among divergent lineages and introgression of adaptive alleles at other loci in the genome. We consider this less likely, given that the X chromosome locus is part of the genetic architecture of local adaptation in most native-range lineages that contributed ancestry to invasive populations. Also, relative to native populations, most invasive populations showed limited evidence of selection at the X chromosome locus, despite varying in ancestry and extent of hybridization. The second explanation is that temporary or permanent changes in selection pressure occurred during biological invasion in *A. sagrei*.

Changes in selection pressure can contribute to differences in hybridization frequency that we observe between ranges. For example, to the extent that dispersal in the native range occurs between populations that are adapted to different environments, natural selection is expected to limit within or among clade gene flow via both premating and postmating mechanisms (40, 41), thereby enhancing population genetic structure. Premating isolation occurs when selection removes maladapted immigrant genotypes before these can produce hybrid offspring (40). Postmating isolation occurs because hybrids are maladapted to the new environment as a result of additive genetic effects when hybrids are intermediate relative to parents, dominant genetic effects when hybrids are mismatched for different parental phenotypes (49), or epistatic genetic effects when interactions among loci create departures from additivity (50).

Epistatic Interactions Occur in Hybrids among Divergent Lineages. The availability of different hybrid genomic backgrounds and detailed trait information in Florida *A. sagrei* allowed us to test if epistasis increases postmating isolation among divergent clades in the native range. Under this scenario, long-term isolation of *A. sagrei* clades led to the random accumulation of divergent alleles genome-wide that interact with alleles at the adaptive X chromosome locus. Thus, two native populations that are adapted to the same environment, but are members of different clades, would still experience limited genetic exchange because hybrids will be maladapted as a result of epistatic interactions between divergent alleles. In the invasive range however, due to changes in selection pressure, hybrids are common and can persist. To test for epistasis, we used genome-wide association (GWA) and included 13 traits that describe the size and shape of lizards (*SI Appendix*, *Supplemental Methods* and Dataset S2). Previous studies have indicated that variation in all these traits might have an adaptive basis in anoles (51), although most support so far has been obtained for limb length (discussed in ref. 25).

The linear-mixed model implemented in GEMMA (52) indicated that SNPs suggestively associated with the length of the distal portion of hindlimb, including metatarsals and phalanges,

map to the same candidate adaptive locus that we identified on the X chromosome (Fig. 3 *A* and *B* and *SI Appendix*, Fig. S23). A stronger and genome-wide significant signal was observed for the same trait at this genomic region using the asaMap association model (53), which allows effect sizes to vary depending on ancestry ($P = 3.40 \times 10^{-7}$) (Fig. 3*A* and *SI Appendix*, Fig. S23). As well, asaMap analyses indicated that the same locus affects variation in several other components of limb length (Fig. 3*A* and *SI Appendix*, Fig. S23). That the same locus is involved in the control of multiple limb components is expected, given the strong positive correlation among these traits across samples, after removing the effect of body size (*SI Appendix*, Fig. S24). Identifying the genes that control variation in limb length in *A. sagrei* is outside the scope of this study. Nonetheless, we note that among the 267 genes that span the 18-Mbp region on the X chromosome, there are several candidate genes known to be involved in limb development. These include *Cut Like Homeobox 2* (*Cux2*) (54), *Growth Differentiation Factor 11* (*GDF11*) (55), *Noggin* (*Nog*) (56), *T-Box Transcription Factor 1* (*Tbx1*) (57), and *Xylosyltransferase 1* (*Xylt1*) (58). In sum, GWA findings indicate that the X chromosome locus singled out by genome scan analyses affects limb length, variation of which is known to be adaptive in anoles (25). These results reinforce our conclusion that positive selection (rather than background selection) is acting at the X chromosome locus and implicate limb length as an important component of adaptive divergence in the native range.

The asaMap analyses further indicated that the strength of association between alleles at the X chromosome locus and limb-length phenotypes vary among the lineages that are hybridizing in Florida. Specifically, for three of the four traits for which the X chromosome locus was the top GWA, an effect was inferred for the western Cuba ancestry component of invasive hybrids (*SI Appendix*, Table S2), but not for the eastern Cuba ancestry component. These results are consistent with epistatic interactions between alleles at the X chromosome limb-length locus and alleles of eastern Cuba origin that are located elsewhere in the genome. While epistasis has traditionally been considered in relation to intrinsic (i.e., unconditional) isolation under the Bateson–Dobzhansky–Muller model (59), evidence has been accumulating for a contribution of such interactions to extrinsic isolation as well (e.g., ref. 50).

To further investigate these results, we stratified the Florida samples based on ancestry into two groups. The first of these consisted of samples with predominantly western Cuba ancestry and low heterozygosity (*SI Appendix*, *Supplemental Methods* and Fig. S25). Therefore, we refer to this group as the "hybridization-limited" group. The second group consisted of samples with ancestry from all parental lineages and high heterozygosity (*SI Appendix*, Fig. S25). Therefore, we refer to these samples as the "hybridization common" group. We then tested for an effect of genotype at the limb-length locus in each of these sample groups. In line with results presented above, when considering samples with limited hybrid ancestry, we detected a large and significant effect of genotype on all limb-length traits but one. Effect sizes in this case ranged from moderate (percent variance explained [PVE] 5.7 to 9.3%) to large (PVE 10.03 to 13.08%) (Fig. 3 *C* and *D*). By contrast, no such effect was observed in the sample group for which hybridization is common (Fig. 3 *C* and *D*).

Similar patterns could arise if hybrid and nonhybrid samples differ with respect to linkage between alleles at the genotyped SNP and the causal limb-length SNP. This may occur in our dataset, given that we used reduced representation sequencing, and therefore are likely not genotyping causal variants. To evaluate this possibility, we repeated these analyses using only samples with western Cuba ancestry at the X chromosome locus (*SI Appendix*, *Supplemental Methods*), reasoning that linkage relationships are more likely to be similar among closely related haplotypes. Results were equivalent to those for the complete dataset, as expected if epistatic interactions rather than linkage disequilibrium underpin differences in effect sizes between hybrid categories (*SI Appendix*, Fig. S26). A limitation of epistasis analyses presented above is that we could not compare the effect of genotype at the limb-length locus in hybrids relative to decidedly nonhybrid *A. sagrei*. This limitation is because pure parental genotypes are rare in Florida. Nonetheless, because of residual hybridization in the hybridization-limited group, the effect sizes that we estimate for these samples may well be conservative.

Phenotype–Environment Correlations Are Consistent with Changes in Natural Selection during Biological Invasion. Previous studies of local adaptation in anoles have relied, among other methods, on phenotype–environment correlations. In the native range, a positive relationship exists both interspecifically and among conspecific populations between the diameter of the perches that anoles use and limb length (reviewed in ref. 25). Biomechanical studies reveal the underlying basis for this relationship, specifically that the optimal limb length for lizard sprint speed and agility is a function of surface diameter (60, 61). Although this relationship has been found repeatedly in natural and experimental *A. sagrei* populations (25, 28, 29), it was not found in a comparison of invasive *A. sagrei* populations in Florida (62).

To investigate whether this lack of a relationship is still the case, we used the 30 populations from Florida and southern Georgia described above for genomic and trait analyses, for which we additionally obtained 1,028 observations of habitat use (Dataset S3). These populations were chosen to avoid heavily disturbed or urban sites, such that nearly all habitat measurements originated from natural vegetation, similar to Kolbe et al. (62). We found the situation to be the same as in the Kolbe et al. (62) study, with no relationship between population average values of relative limb length and perch diameter ($R^2 = 4.61 \times 10^{-5}$; $P = 0.97$) (*SI Appendix*, Fig. S27). Thus, results from phenotype–environment correlation analyses are consistent with genomic results above, indicating that changes in natural selection occurred during biological invasion in *A. sagrei*. We note, however, that a caveat of these analyses is that native populations used in previous studies are predominantly from islands in the Bahamas (25, 28, 29). Comparable data from Cuban populations that sourced the Florida invasion are currently not available.

Conclusions

Our results indicate that changes in natural selection as inferred from genomic variation at a large-effect adaptive X chromosome locus contribute to differences in hybridization frequency among native and invasive populations of *A. sagrei*. In the native range, evidence of frequent selective sweeps suggests that the X chromosome locus, which affects variation in limb length, is an important component in the adaptive response of *A. sagrei* populations to the environment. To the extent that migration occurs among contrasting environments in the native range, adaptive divergence could limit gene flow among populations within or between clades. Ancestry-specific association analyses, which we could perform thanks to the availability of invasive hybrids, additionally showed that the same X chromosome locus is involved in epistatic interactions when hybridization occurs among divergent lineages. This result indicates that native range extrinsic isolation may be stronger between populations from different clades and provides an example on the value of studying invasive populations for understanding evolution in the native range.

Although *A. sagrei* has been reasonably well sampled across its range in Cuba, more detailed study of the contact zones between clades is needed. Combining genomic data with trait and habitat data will provide in-depth information on native range gene flow and environmental drivers of local adaptation. In the invasive range, natural selection as it is manifested in the native range, appears to have been disrupted. Here, hybrid ancestry occurs in

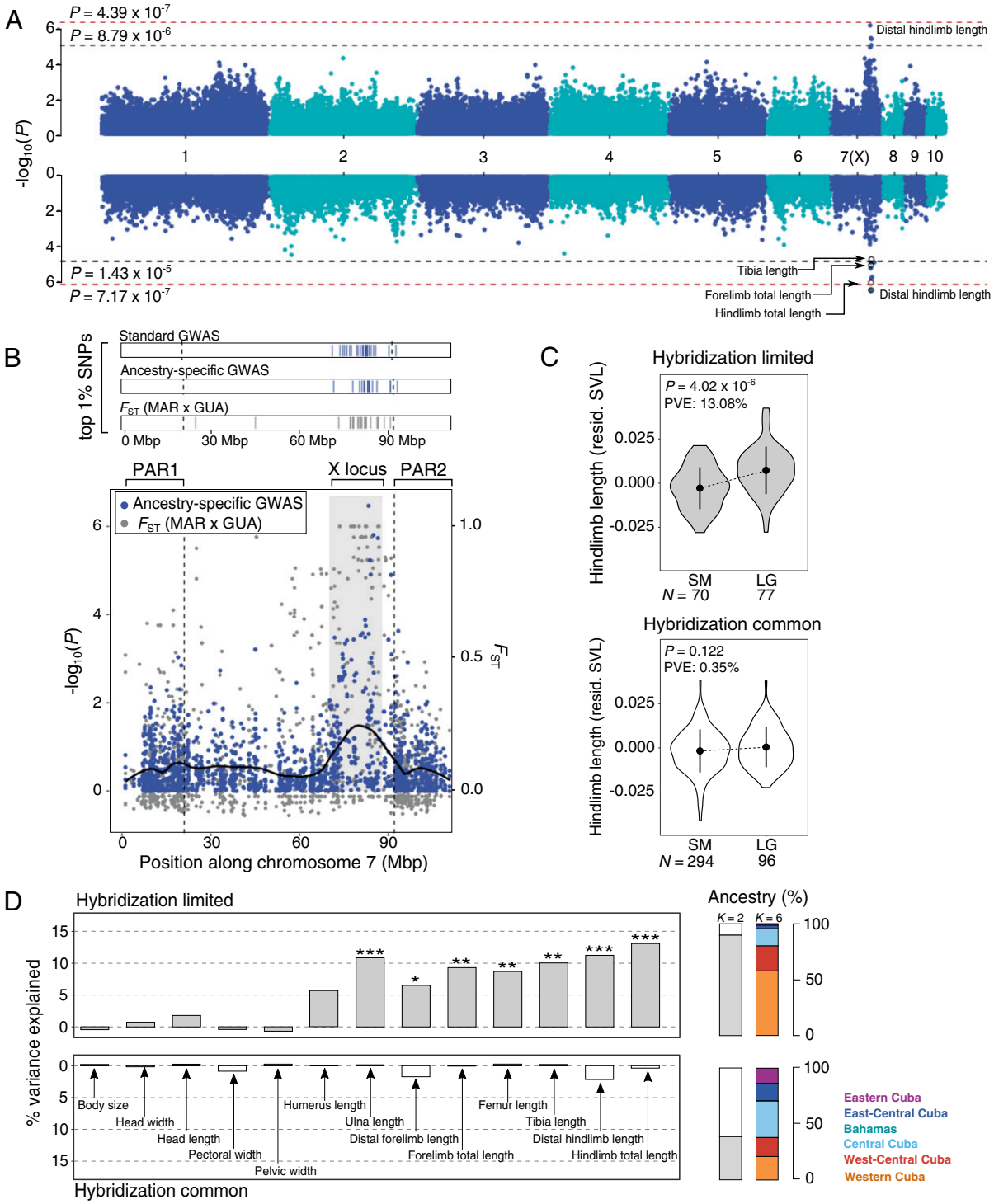

Fig. 3. Genetic architecture of limb length. (*A*) GWAs for the relative length of the distal portion of hindlimb, inferred using the GEMMA association model (*Upper*) and the asaMap ancestry-specific association model (*Lower*). For the asaMap results, white dots show the smallest *P* values for three other traits for which the same locus was identified as the top GWA (see *SI Appendix*, Fig. S23 for GWA results for each trait). The red dashed lines are the Bonferroni-corrected significance thresholds, while the black dashed lines indicate the suggestive significance thresholds (*SI Appendix*, *Supplemental Methods*). (*B*) Overlap between GWA for limb length and F_{ST} outliers in the native range. The *Upper* plot indicates, for chromosome 7, the position of the top 1% SNPs identified based on strength of GWA (blue lines) or F_{ST} (gray lines). F_{ST} values are from the Mariel × Guanabo population pair (*SI Appendix*, Fig. S12). The lower plot shows asaMap association results (blue dots), and Mariel × Guanabo F_{ST} values per SNP (gray dots) along chromosome 7. The black line is a loess smoothing ("span" of 0.2) of association results. The gray shading marks the 18-Mbp X chromosome divergent locus, and the dashed vertical lines indicate the boundaries of the two PARs on the X chromosome. (*C*) Relative hindlimb length for samples with small (SM) and large (LG) alleles at the lead SNP identified on chromosome 7 using the asaMap model. Trait values are given separately for the hybridization-limited and the hybridization common sample groups. Points and error bars indicate mean and SD. (*D*) Effect sizes of genotypes at the same SNP as in *C*, calculated for all traits, for each of the two sample groups separately. Asterisks indicate significant main effects of genotype after Bonferroni correction. *$P < 0.05$; **$P < 0.01$; ***$P < 0.001$. For each sample group, ancestry proportions are shown as estimated using a STRUCTURE analysis at $K = 2$ and $K = 6$ (see also *SI Appendix*, Fig. S25).

all populations and has stabilized irrespective of whether gene flow occurred within or among divergent lineages.

Whether hybridization had a major role in the success of the *A. sagrei* invasion remains to be definitively established. Nonetheless, available evidence points toward hybridization-mediated biological invasion. Specifically, hybrid ancestry occurs in all invasive populations. Were hybridization merely a consequence of repeated introductions, we would have expected to find a mosaic of hybrid and nonhybrid ancestry across the invasive range. Aside from being widespread, hybrid ancestry has stabilized: samples collected 15 y apart, while representing a narrow snapshot in the history of invasive *A. sagrei*, did not reveal changes in ancestry. Thus, even if currently neutral, stability of new ancestry combinations should increase the chance that adaptive allele combinations are available when invasive populations are exposed to novel selective pressures.

Methods

Sequencing and Variant Calling. To obtain genome-wide SNP data, we used ddRADseq (*SI Appendix, Supplemental Methods*). We aligned quality-filtered reads to the *A. sagrei* reference genome v2.0 (63, 64) in the dDocent v2.2.20 pipeline (65). We then performed joint genotyping using Freebayes v1.3.2 (66), including data from the 897 *A. sagrei* libraries (885 samples and 12 replicates), along with 128 other *A. sagrei* libraries that were part of a related project. To decrease SNP calling runtime and following Freebayes manual recommendations, we only called the six best alleles. We next applied stringent variant filtering and estimated postfiltering genotyping errors (*SI Appendix, Supplemental Methods*).

Spatial Population Genetic Structure across the Range of *A. sagrei*. To summarize population structure, we used PCA in "adegenet" (v2.1.1) (67). Fine-scale population structure in western Cuba was explored using a separate PCA. For each analysis, we identified markers genotyped in at least 99% of samples with a minor allele frequency > 1%. From this set, to decrease computational time, we selected 10,000 random SNPs using the "vcfrandomsample" tool from *vcflib* (https://github.com/vcflib/vcflib). These SNPs were located on chromosomes 1 to 5 of the v2.0 reference genome, which are equivalent to chromosomes 1 to 6 of the v2.1 reference genome (63, 64). For consistency, we will refer only to genome coordinates v2.1 throughout. We complemented the PCA with estimates of the *A. sagrei* phylogeny, Bayesian clustering, identity-by-state, and IBD (*SI Appendix, Supplemental Methods*).

Temporal Changes in the Ancestry of Invasive Hybrids. To investigate whether the ancestry of invasive hybrids has stabilized or is changing, we revisited in 2018 six populations that we sampled in 2003 ($n = 172$) (*SI Appendix*, Fig. S9). We targeted the same sites, or sites located as close as possible to the original 2003 sampling. We first used PCA, as described above. Additionally, we modeled temporal changes at three metrics of hybrid status, as follows. First, we identified a set of ancestry informative markers (AIMs) that are diagnostic of the western Cuba lineage. To be classified as AIMs, SNPs needed to be scored in 70% or more of western Cuba and nonwestern Cuba samples, and show an allele frequency of 20% or lower in one group, and 80% or higher in the other. In all, 711 SNPs fit these criteria, of which 469 were scored at high quality in the 2003 and 2018 invasive samples. To summarize western Cuba ancestry, we then averaged AIM allele frequency for each invasive genotype.

Second, we calculated an index of admixture (H_A), following Keller and Taylor (12). As input, we used the STRUCTURE results from the $K = 6$ analysis with prior population information (Fig. 1*B*). Third, we calculated heterozygosity using 155,905 filtered SNPs from chromosomes 1 to 6 (for details on SNP filtering, see identity-by-state analyses section in *SI Appendix, Supplemental Methods*). To test whether AIM allele frequency, H_A, or heterozygosity changed over 15 y, we used three linear models in R v3.6.1 (68). These had each of the three metrics as the response variable, and population IDs and time (2003 or 2018) as the predictor variable.

The Genomic Signature of Natural Selection in *A. sagrei*. We combined information from relative differentiation (F_{ST}), Tajima's *D*, Fay and Wu's *H* test, nucleotide diversity (π), and absolute differentiation (D_{xy}). For the invasive range, we used the 30 populations sampled in 2018 from Florida and southern Georgia ($n = 560$) (Dataset S1). For the native range, we used all 10 populations ($n = 134$) (Dataset S1). Prior to performing analyses along the genome, we updated genome coordinates from v2.0, which was used to align reads and call SNPs to the most recent version (v2.1), which includes changes to sequence coordinates but does not differ in sequence content. We then removed gametolog SNPs (i.e., SNPs resulting from Y chromosome reads that align to the X chromosome) (*SI Appendix, Supplemental Methods*), and imputed any missing data at the remaining 123,882 SNPs in BEAGLE v5.0 (69).

For F_{ST} analyses, we used population pairwise comparisons and calculated F_{ST} in nonoverlapping windows of 50 kb in VCFtools (v0.1.16) (70). To avoid pseudoreplication, we used only unique population pairs (see *SI Appendix, Supplemental Methods* for details on population pairing). We then classified windows as "outliers" if weighted F_{ST} was in the top 5% of observations (i.e., we sorted windowed F_{ST} for each population pair, and obtained windows in the top 5%). Similarly, "extreme outliers" were windows in the top 1%. Aside from evaluating how F_{ST} varies along the genome, this approach additionally allowed us to investigate the repeatability of F_{ST} differentiation, using a permutation approach implemented from Rennison et al. (71) (*SI Appendix, Supplemental Methods*).

Tajima's *D* was calculated in nonoverlapping windows of 50 kb in VCFtools. To estimate Fay and Wu's *H*, we used "PopGenome" (v2.7.5) (72). We first incorporated an outgroup from publicly available sequence data (*SI Appendix, Supplemental Methods*), retaining 139 SNPs scored at the divergent X chromosome locus for all samples and for the outgroup. To get an estimate of background neutral *H* values at the X chromosome, we obtained another set of 139 SNPs with outgroup data. Similar to SNPs from the divergent X chromosome locus, these were located in the male-hemizygous region, between pseudoautosomal region 1 (PAR1) and PAR2. To minimize effects of genetic hitchhiking that would extend the signature of selection in the vicinity of an adaptive locus, candidate neutral SNPs were from the opposite end of the X chromosome (i.e., adjacent to PAR1). We then compared *H* values obtained for each range at the divergent X chromosome locus to neutral values, and for each locus category between ranges, using Wilcoxon rank-sum tests in R, adjusting *P* values for multiple comparisons using the Bonferroni method. Finally, while analyses of selection focused on the 2018 invasive range samples, we also contrasted *H* values between the 2003 and 2018 samples for the six invasive populations with temporal data. To do this, we followed the same approach as described above for the full dataset.

To calculate nucleotide diversity (π), and absolute differentiation (D_{xy}), we repeated the SNP calling step for the X chromosome, retaining monomorphic sites as well. We filtered the output, keeping genotypes supported by at least four reads and sites with data in at least 70% of samples used for the genome scan analyses. Also, we removed gametolog SNPs using the same approach as for the 123,882 SNP set described above, used in the rest of the genome scan analyses (see also *SI Appendix, Supplemental Methods*). We then used the python script "popgenWindows.py" (https://github.com/simonhmartin/genomics_general) (73) to estimate π and D_{xy} in nonoverlapping windows of 50 kb along the X chromosome, based on windows with at least 50 sites with data. For D_{xy}, we used the same pairs of populations as in the F_{ST} analyses. We compared average per population π from within the divergent X chromosome locus (107 windows) to a candidate neutral locus of the same size (107 windows) using the same approach as for Fay and Wu's *H* test above.

Genetic Mapping of Candidate Adaptive Traits in Natural Hybrid Populations. We measured 13 morphological traits that describe body size (SVL), as well as the shape of lizards using image analysis of X-rays (*SI Appendix, Supplemental Methods* and Dataset S2). Measurements at skeletal traits were isolated from the effect of SVL by calculating residuals from linear regressions of log-transformed trait values on log-transformed SVL in R. Two GWA approaches were then used: a linear-mixed model in GEMMA (52) and ancestry-specific association in asaMap (53). Both analyses were based on the samples obtained in 2018 from Florida and southern Georgia ($n = 560$). We filtered a VCF containing these 560 samples using the same criteria as above. As well, similar to the genome scan analyses, we removed gametolog SNPs and imputed any missing data that remained after filtering. For the GEMMA analyses, we used a leave-one-chromosome-out approach when calculating the relatedness matrix. For the asaMap analyses, to account for population structure, we included as covariates the first 10 PCs from a PCA constructed in "adegenet" for all samples in the analysis. Also, for both GWA approaches, we included transect as an additional covariate (see *SI Appendix, Supplemental Methods* for additional details).

Data Availability. All raw sequence data used in this study are stored in the Sequence Read Archive (SRA), https://www.ncbi.nlm.nih.gov/sra (BioProject accession PRJNA737437). SRA accession numbers for each sample are given in Dataset S1. Additional files related to the reference genome are archived on Harvard Dataverse (64), https://doi.org/10.7910/DVN/TTKBFU. Trait data are available in Dataset S2 and habitat data are available in Dataset S3.

Additionally, the specimens used to collect trait data along with the associated X-ray images have been deposited in the Herpetological Collection of the Harvard Museum of Comparative Zoology (museum identification codes are given in Dataset S1). Back-up tissue samples for these specimens are maintained in the cryogenic collection at the Harvard Museum of Comparative Zoology. Code used in the analyses, filtered SNP datasets, and other analysis-related files are available on Dryad (74), https://doi.org/10.5061/dryad.hdr7sqvjg.

ACKNOWLEDGMENTS. We thank K. A. Hodgins, L. H. Rieseberg, and the J.B.L. and J.J.K. laboratories for helpful comments, as well as J. Breeze, C. Hahn, and M. Gage for assistance with lizard housing and care. This work was made possible by a Natural Sciences and Engineering Research Council of Canada Postdoctoral Fellowship, a Banting Postdoctoral Fellowship, and a Barbour award from the Harvard Museum of Comparative Zoology (to D.G.B.); National Science Foundation Grant DEB-1927194 (to A.J.G. and J.B.L.); NSF Grant IOS-1827647 (to D.B.M.); and NSF Grant DEB-1354897 and funds from the University of Rhode Island (to J.J.K.). Additionally, this project was made possible through the support of a grant from the John Templeton Foundation. The opinions expressed in this publication are those of the authors and do not necessarily reflect the views of the John Templeton Foundation.

1. H. G. Baker, G. L. Stebbins, *The Genetics of Colonizing Species* (Academic, New York, 1965).
2. C. E. Lee, Evolutionary genetics of invasive species. *Trends Ecol. Evol.* **17**, 386–391 (2002).
3. S. L. Chown *et al*., Biological invasions, climate change and genomics. *Evol. Appl.* **8**, 23–46 (2015).
4. D. G. Bock *et al*., What we still don't know about invasion genetics. *Mol. Ecol.* **24**, 2277–2297 (2015).
5. R. I. Colautti, J. A. Lau, Contemporary evolution during invasion: Evidence for differentiation, natural selection, and local adaptation. *Mol. Ecol.* **24**, 1999–2017 (2015).
6. N. G. Hairston, S. P. Ellner, M. A. Geber, T. Yoshida, J. A. Fox, Rapid evolution and the convergence of ecological and evolutionary time. *Ecol. Lett.* **8**, 1114–1127 (2005).
7. D. N. Reznick, J. Losos, J. Travis, From low to high gear: There has been a paradigm shift in our understanding of evolution. *Ecol. Lett.* **22**, 233–244 (2019).
8. R. J. Abbott, Plant invasions, interspecific hybridization and the evolution of new plant taxa. *Trends Ecol. Evol.* **7**, 401–405 (1992).
9. N. C. Ellstrand, K. A. Schierenbeck, Hybridization as a stimulus for the evolution of invasiveness in plants? *Proc. Natl. Acad. Sci. U.S.A.* **97**, 7043–7050 (2000).
10. M. Rius, J. A. Darling, How important is intraspecific genetic admixture to the success of colonising populations? *Trends Ecol. Evol.* **29**, 233–242 (2014).
11. J. J. Kolbe *et al*., Genetic variation increases during biological invasion by a Cuban lizard. *Nature* **431**, 177–181 (2004).
12. S. R. Keller, D. R. Taylor, Genomic admixture increases fitness during a biological invasion. *J. Evol. Biol.* **23**, 1720–1731 (2010).
13. D. G. Bock, M. B. Kantar, C. Caseys, R. Matthey-Doret, L. H. Rieseberg, Evolution of invasiveness by genetic accommodation. *Nat. Ecol. Evol.* **2**, 991–999 (2018).
14. H. S. Rosinger *et al*., The tip of the iceberg: Genome wide marker analysis reveals hidden hybridization during invasion. *Mol. Ecol.* **30**, 810–825 (2021).
15. S. M. Hovick, K. D. Whitney, Hybridisation is associated with increased fecundity and size in invasive taxa: Meta-analytic support for the hybridisation-invasion hypothesis. *Ecol. Lett.* **17**, 1464–1477 (2014).
16. K. D. Whitney, R. A. Randell, L. H. Rieseberg, Adaptive introgression of herbivore resistance traits in the weedy sunflower *Helianthus annuus*. *Am. Nat.* **167**, 794–807 (2006).
17. A. Zhan, H. J. Macisaac, M. E. Cristescu, Invasion genetics of the *Ciona intestinalis* species complex: From regional endemism to global homogeneity. *Mol. Ecol.* **19**, 4678–4694 (2010).
18. E. Anderson, Hybridization of the habitat. *Evolution* **2**, 1–9 (1948).
19. M. Todesco *et al*., Hybridization and extinction. *Evol. Appl.* **9**, 892–908 (2016).
20. B. R. Grant, P. R. Grant, Evolution of Darwin finches caused by a rare climatic event. *Proc. Biol. Sci.* **251**, 111–117 (1993).
21. C. B. Heiser, Hybrid populations of *Helianthus divaricatus* and *H. microcephalus* after 22 years. *Taxon* **28**, 71–75 (1979).
22. K. J. F. Verhoeven, M. Macel, L. M. Wolfe, A. Biere, Population admixture, biological invasions and the balance between local adaptation and inbreeding depression. *Proc. Biol. Sci.* **278**, 2–8 (2011).
23. K. L. Millette, A. Gonzalez, M. E. Cristescu, Breaking ecological barriers: Anthropogenic disturbance leads to habitat transitions, hybridization, and high genetic diversity. *Sci. Total Environ.* **740**, 140046 (2020).
24. J. J. Kolbe, A. Larson, J. B. Losos, K. de Queiroz, Admixture determines genetic diversity and population differentiation in the biological invasion of a lizard species. *Biol. Lett.* **4**, 434–437 (2008).
25. J. B. Losos, *Lizards in an Evolutionary Tree: Ecology and Adaptive Radiation of Anoles* (University of California Press, Berkeley, CA, 2009).
26. B. C. Lister, The nature of niche expansion in West Indian *Anolis* lizards I: Ecological consequences of reduced competition. *Evolution* **30**, 659–676 (1976a).
27. B. C. Lister, The nature of niche expansion in West Indian *Anolis* lizards II: Evolutionary components. *Evolution* **30**, 677–692 (1976b).
28. J. B. Losos, D. J. Irschick, T. W. Schoener, Adaptation and constraint in the evolution of specialization of Bahamian *Anolis* lizards. *Evolution* **48**, 1786–1798 (1994).
29. J. B. Losos, K. I. Warheitt, T. W. Schoener, Adaptive differentiation following experimental island colonization in *Anolis* lizards. *Nature* **387**, 70–73 (1997).
30. J. J. Kolbe, M. Leal, T. W. Schoener, D. A. Spiller, J. B. Losos, Founder effects persist despite adaptive differentiation: A field experiment with lizards. *Science* **335**, 1086–1089 (2012).
31. R. M. Cox, R. Calsbeek, Survival of the fattest? Indices of body condition do not predict viability in the brown anole (*Anolis sagrei*). *Funct. Ecol.* **29**, 404–413 (2015).
32. O. Lapiedra, T. W. Schoener, M. Leal, J. B. Losos, J. J. Kolbe, Predator-driven natural selection on risk-taking behavior in anole lizards. *Science* **360**, 1017–1020 (2018).
33. R. M. Pringle *et al*., Predator-induced collapse of niche structure and species coexistence. *Nature* **570**, 58–64 (2019).
34. I. J. Wang, R. E. Glor, J. B. Losos, Quantifying the roles of ecology and geography in spatial genetic divergence. *Ecol. Lett.* **16**, 175–182 (2013).
35. R. G. Reynolds *et al*., Phylogeographic and phenotypic outcomes of brown anole colonization across the Caribbean provide insight into the beginning stages of an adaptive radiation. *J. Evol. Biol.* **33**, 468–494 (2020).
36. P. G. Meirmans, The trouble with isolation by distance. *Mol. Ecol.* **21**, 2839–2846 (2012).
37. R. E. Glor *et al*., Partial island submergence and speciation in an adaptive radiation: A multilocus analysis of the Cuban green anoles. *Proc. Biol. Sci.* **271**, 2257–2265 (2004).
38. A. F. Agrawal, M. C. Whitlock, Environmental duress and epistasis: How does stress affect the strength of selection on new mutations? *Trends Ecol. Evol.* **25**, 450–458 (2010).
39. J. M. Coughlan, D. R. Matute, The importance of intrinsic postzygotic barriers throughout the speciation process. *Philos. Trans. R. Soc. Lond. B Biol. Sci.* **375**, 20190533 (2020).
40. P. Nosil, T. H. Vines, D. J. Funk, Perspective: Reproductive isolation caused by natural selection against immigrants from divergent habitats. *Evolution* **59**, 705–719 (2005).
41. A. P. Hendry, P. Nosil, L. H. Rieseberg, The speed of ecological speciation. *Funct. Ecol.* **21**, 455–464 (2007).
42. K. A. Hodgins, D. G. Bock, L. H. Rieseberg, Trait evolution in invasive species. *Annu. Plant Rev. Online* **1**, 1–37 (2018).
43. R. Nielsen, Molecular signatures of natural selection. *Annu. Rev. Genet.* **39**, 197–218 (2005).
44. K. E. Lohmueller, C. D. Bustamante, A. G. Clark, Detecting directional selection in the presence of recent admixture in African-Americans. *Genetics* **187**, 823–835 (2011).
45. P. C. Sabeti *et al*., Positive natural selection in the human lineage. *Science* **312**, 1614–1620 (2006).
46. R. Burri, Interpreting differentiation landscapes in the light of long-term linked selection. *Evol. Lett.* **1**, 118–131 (2017).
47. D. E. Irwin *et al*., A comparison of genomic islands of differentiation across three young avian species pairs. *Mol. Ecol.* **27**, 4839–4855 (2018).
48. T. E. Cruickshank, M. W. Hahn, Reanalysis suggests that genomic islands of speciation are due to reduced diversity, not reduced gene flow. *Mol. Ecol.* **23**, 3133–3157 (2014).
49. K. A. Thompson, M. Urquhart-Cronish, K. D. Whitney, L. H. Rieseberg, D. Schluter, Patterns, predictors, and consequences of dominance in hybrids. *Am. Nat.* **197**, E72–E88 (2021).
50. J. R. Dettman, C. Sirjusingh, L. M. Kohn, J. B. Anderson, Incipient speciation by divergent adaptation and antagonistic epistasis in yeast. *Nature* **447**, 585–588 (2007).
51. L. J. Harmon, J. J. Kolbe, J. M. Cheverud, J. B. Losos, Convergence and the multidimensional niche. *Evolution* **59**, 409–421 (2005).
52. X. Zhou, M. Stephens, Genome-wide efficient mixed-model analysis for association studies. *Nat. Genet.* **44**, 821–824 (2012).
53. L. Skotte, E. Jørsboe, T. S. Korneliussen, I. Moltke, A. Albrechtsen, Ancestry-specific association mapping in admixed populations. *Genet. Epidemiol.* **43**, 506–521 (2019).
54. A. T. Tavares, T. Tsukui, J. C. Izpisúa Belmonte, Evidence that members of the Cut/Cux/CDP family may be involved in AER positioning and polarizing activity during chick limb development. *Development* **127**, 5133–5144 (2000).
55. Y. Matsubara *et al*., Anatomical integration of the sacral-hindlimb unit coordinated by GDF11 underlies variation in hindlimb positioning in tetrapods. *Nat. Ecol. Evol.* **1**, 1392–1399 (2017).
56. K. Lehmann *et al*., A new subtype of brachydactyly type B caused by point mutations in the bone morphogenetic protein antagonist NOGGIN. *Am. J. Hum. Genet.* **81**, 388–396 (2007).
57. G. Tejedor *et al*., Whole embryo culture, transcriptomics and RNA interference identify TBX1 and FGF11 as novel regulators of limb development in the mouse. *Sci. Rep.* **10**, 3597 (2020).
58. E. K. Mis *et al*., Forward genetics defines Xylt1 as a key, conserved regulator of early chondrocyte maturation and skeletal length. *Dev. Biol.* **385**, 67–82 (2014).
59. J. A. Coyne, H. A. Orr, *Speciation* (Sinauer Associates) 2004).
60. J. B. Losos, B. Sinervo, The effects of morphology and perch diameter on sprint performance of *Anolis* lizards. *J. Exp. Biol.* **145**, 23–30 (1989).
61. B. Vanhooydonck, A. Herrel, D. J. Irschick, Out on a limb: The differential effect of substrate diameter on acceleration capacity in *Anolis* lizards. *J. Exp. Biol.* **209**, 4515–4523 (2006).
62. J. J. Kolbe, A. Larson, J. B. Losos, Differential admixture shapes morphological variation among invasive populations of the lizard *Anolis sagrei*. *Mol. Ecol.* **16**, 1579–1591 (2007).

63. A. J. Geneva *et al*., Chromosome-scale genome assembly of the brown anole (*Anolis sagrei*), a model species for evolution and ecology. *bioRxiv [Preprint]*, https://doi.org/10.1101/2021.09.28.462146 (Accessed 30 September 2021).
64. A. J. Geneva *et al*., Chromosome-scale genome assembly of the brown anole (Anolis sagrei), a model species for evolution and ecology. *Harvard Dataverse*. https://doi.org/10.7910/DVN/TTKBFU. Deposited 30 September 2021.
65. J. B. Puritz, C. M. Hollenbeck, J. R. Gold, dDocent: A RADseq, variant-calling pipeline designed for population genomics of non-model organisms. *PeerJ* **2**, e431 (2014).
66. E. Garrison, G. Marth, Haplotype-based variant detection from short-read sequencing. arXiv [Preprint] (2012). https://arxiv.org/abs/1207.3907 (Accessed 20 July 2012).
67. T. Jombart, I. Ahmed, adegenet 1.3-1: New tools for the analysis of genome-wide SNP data. *Bioinformatics* **27**, 3070–3071 (2011).
68. R Development Core Team, *R: A Language and Environment for Statistical Computing* (www.R-project.org/) (R Foundation for Statistical Computing, 2011).
69. B. L. Browning, S. R. Browning, Genotype imputation with millions of reference samples. *Am. J. Hum. Genet.* **98**, 116–126 (2016).
70. P. Danecek *et al*.; 1000 Genomes Project Analysis Group, The variant call format and VCFtools. *Bioinformatics* **27**, 2156–2158 (2011).
71. D. J. Rennison, Y. E. Stuart, D. I. Bolnick, C. L. Peichel, Ecological factors and morphological traits are associated with repeated genomic differentiation between lake and stream stickleback. *Philos. Trans. R. Soc. Lond. B Biol. Sci.* **374**, 20180241 (2019).
72. B. Pfeifer, U. Wittelsbürger, S. E. Ramos-Onsins, M. J. Lercher, PopGenome: An efficient Swiss army knife for population genomic analyses in R. *Mol. Biol. Evol.* **31**, 1929–1936 (2014).
73. S. H. Martin, J. W. Davey, C. D. Jiggins, Evaluating the use of ABBA-BABA statistics to locate introgressed loci. *Mol. Biol. Evol.* **32**, 244–257 (2015).
74. D. G. Bock *et al*., Changes in selection pressure can facilitate hybridization during biological invasion in a Cuban lizard. *Dryad*. https://doi.org/10.5061/dryad.hdr7sqvjg. Deposited 30 September 2021.